Eashika Ghosh, Aleksandr I. Egunov*, Daniil Karnaushenko, Mariana Medina-Sánchez* and Oliver G. Schmidt

Self-assembled sensor-in-a-tube as a versatile tool for label-free EIS viability investigation of cervical cancer cells

https://doi.org/10.1515/freq-2022-0090
Received April 26, 2022; accepted October 5, 2022;
published online October 24, 2022

Abstract: The advancement of micro and nanotechnology has led to the manufacturing of miniaturized sensors with improved functionalities for highly sensitive point of care devices. This work is particularly focused on analysing cancer cells and the effect of a model drug on their survival rate. To that end, we developed a highly sensitive rolled-up micro-electrochemical impedance spectroscopy sensor, encapsulated into a microfluidic channel. The sensor was built by strain engineering of shapeable materials and with diameters close to the cell size to improve their sensitivity. To demonstrate the platform performance, we first carried out measurements with different electrode geometries using cell medium at different concentrations. We also performed measurements using cancer cell suspensions, obtaining distinct signals from single cells, cell clusters and cellular debris. Finally, cancer cells were treated with an anticancer drug (Camptothecin), at different concentrations, over the same period, and further analysed using the developed platform.

Keywords: electrical impedance spectroscopy; lab-in-a-tube; label-free impedimetric sensor; shapeable materials technologies; single-cell analysis.

***Corresponding authors: Aleksandr I. Egunov**, Institute for Integrative Nanosciences, Leibniz IFW Dresden, Helmholtzstraße 20, 01069, Dresden, Germany; and Research Center for Materials, Architectures and Integration of Nanomembranes, Chemnitz University of Technology, Rosenbergstraße 6, 09126, Chemnitz, Germany, E-mail: aleksandr.egunov@main.tu-chemnitz.de. https://orcid.org/0000-0002-7077-8817; and **Mariana Medina-Sánchez**, Institute for Integrative Nanosciences, Leibniz IFW Dresden, Helmholtzstraße 20, 01069, Dresden, Germany; and Center for Molecular Bioengineering (B CUBE), Dresden University of Technology, Tatzberg 41, 01307, Dresden, Germany, E-mail: m.medina.sanchez@ifw-dresden.de
Eashika Ghosh, Institute for Integrative Nanosciences, Leibniz IFW Dresden, Helmholtzstraße 20, 01069, Dresden, Germany
Daniil Karnaushenko, Institute for Integrative Nanosciences, Leibniz IFW Dresden, Helmholtzstraße 20, 01069, Dresden, Germany; and Research Center for Materials, Architectures and Integration of Nanomembranes, Chemnitz University of Technology, Rosenbergstraße 6, 09126, Chemnitz, Germany
Oliver G. Schmidt, Research Center for Materials, Architectures and Integration of Nanomembranes, Chemnitz University of Technology, Rosenbergstraße 6, 09126, Chemnitz, Germany; Material Systems for Nanoelectronics, Chemnitz University of Technology, Str. der Nationen 62, 09111, Chemnitz, Germany; and Nanophysics, Dresden University of Technology, Haeckelstraße 3, 01069, Dresden, Germany

1 Introduction

Cervical cancer (CC) is the fourth most common cancer among women worldwide [1]. According to the world health organization, in 2020, an estimated 604 000 women were diagnosed with cervical cancer worldwide and about 342 000 women died from the disease [2]. Early diagnosis of CC accelerates therapeutic treatments and significantly contributes to lifesaving. It has been observed that an early detection of cancer would increase the possibilities of treatment success, avoiding to reach to the metastasis stage. The way cervical cancer is diagnosed in human papillomavirus positive women is through biopsy, available imaging techniques, or antibody response analysis [3]. These methods are quite bulky, require specialized personal as well as high volumes of expensive and delicate reagents making CC early diagnosis less accessible in remote regions. Therefore, it is essential to develop robust and reliable diagnosis tools that allow the early detection of CC with low costs and high accessibility. On another hand, it is imperative not only to detect cancer cells at an early stage but also to monitor their behaviour under an applied therapy in a personalized fashion. Personalized medicine is aimed to create or apply therapy according to patient-specific needs. This will make the current therapies with anti-cancer drugs more effective, as there exists a high heterogenicity among the cell population within different patients [4]. The investigation of the anti-cancer drug treatment impact on the cell viability i.e. apoptosis and necrosis, is still challenging at the single cell level. One of the most well-known anti-cancer drugs with proven effectiveness and, however, very limited applications is

Camptothecin. Camptothecin act as topoisomerase inhibitor, enzymes that play an important role in cell reproduction. However, it has very limited use in anti-cancer therapy due to the high toxicity effects towards healthy cells [5]. Therefore, investigation of cancer cell viability could help to find the cause of the high toxicity of drug agents in cancer patients and to find the optimal dose with limited adverse effects.

Analysis of cancer cells on single cell level with high efficiency requires a micro total analysis system (μ-TAS) or a dedicated lab-on-a-chip (LOC). These systems have outstanding advantages such as low sample consumption, rapid analysis, and the possibility to create portable and simple-to-use point of care devices [6]. μ-TAS and LOC devices are fully equipped with highly efficient functional components capable of acquiring results by separating and detecting various samples. Integrated into microfluidic networks, these biosensors or transducers provide additional benefits: low volume of reagents and samples consumption, and close interaction of analytes and cells to the system transducers, thus increasing sensitivity [7]. Microfluidics' integration also improved the method with respect to easier and faster diffusive mass transport and heat conduction [8]. Moreover, microfluidic integration allows in-flow detection of different biological samples, cell counting and cell sorting. Many of recent microfluidic μ-TAS and LOC systems for biological applications rely on electrical detection methods [9], employing transistors or electrodes as transducers, because they offer sensitive quantitative data as well as are susceptible to mass production and miniaturization. Such transducers can be fabricated by different conventional methods such as screen printing [10], inkjet printing [11], photolithography processes [12], among others, being compatible with the fabrication technology of microfluidic channels. One of the most commonly used electrical methods is electrical impedance spectroscopy (EIS) which allows label-free and multi-frequency analysis. EIS devices are programmed to convert the biological samples' responses into a readable physical signal. They can be functionalized with bioreceptors for specific recognition of numerous biological samples, ranging from biomolecules (proteins, DNA, RNA) to single cells and even to tissues [13–17], or can be used without functionalization, by detecting other factors such as cell morphology, cell and extracellular matrix conductivity changes.

In particular, single-cell analysis using microelectrodes is quite promising as the scale in which these systems are fabricated, are typically in the same scale size as single cells. It has also been observed that the microelectrode configuration of the device influences the sensitivity of the EIS based LOC devices. Different layouts of microelectrodes such as coplanar [18], side wall [19], trapezoidal [20], top-bottom [21], interdigitated [22] have been demonstrated for highly accurate and sensitive analysis of single cells [23]. Moreover, there are a few examples where parallel electrodes have been fabricated into microfluidic channel's due to the complex and long fabrication process [21].

Nowadays, a particular attention is paid on the design and fabrication of 3D tubular microelectrode systems. Such tubular microelectrodes are fabricated by transforming two-dimensional electrodes layout to three-dimensional structures by making use of strain engineering, which allows the tunability of the size for fitting cell size. This concept paved the way to the emergence of the lab in a tube concept [24, 25]. The tubular electrode configuration enhances the sensing capabilities in microfluidic devices as the sensing surface per fluid volume increases, favouring the signal coupling with the sample's detection volume. These microtubular electrodes have showed two orders of higher sensitivity in the in-flow detection of mono- and divalent ionic species, providing a limit of detection as 0.1 nM KCl and also showed the ability to detect single HeLa dynamically [26]. Similarly, the microtubular DNA biosensor showed higher sensitivity of four orders of magnitude than their planar counterparts, achieving attomolar detection levels of Avian Influenza Virus H1N1 DNA without amplification or labelling [27]. Likewise, a semiconductor-based microtubular structure showed high sensitivity with respect to coplanar electrodes, being capable of distinguishing between polystyrene beads, primary mouse T lymphocytes, and Jurkat T lymphocytes [28]. A similar work has been done to detect single T-cells and their expressed cytokines with platinum microtubular electrodes, achieving high throughput and enabling the determination of different cell activation stages upon liposaccharides stimuli [29]. As a follow-up application, in the present work, a direct ultrasensitive sensor-in-a-tube is designed to monitor the cell viability and the impact of a model drug on the cells, towards rapid drug screening and personalized medicine applications.

The proposed sensor-in-a-tube (Figure 1) consists of multiple 3D platinum microelectrodes, patterned onto a polymeric layer which is then rolled-up forming a microtube, and embedded into a polydimethylsiloxane (PDMS) microfluidic channel for further sample handling and detection. Initially, the planar stack is processed using conventional parallel photolithography and thin-film deposition methods, resulting in three polymer layers stack. The tubular microelectrode structure reduces the leakage current propagating through the extracellular medium due to the increase in surface to volume ratio, and the possibility to adjust the tube diameter to the cell size.

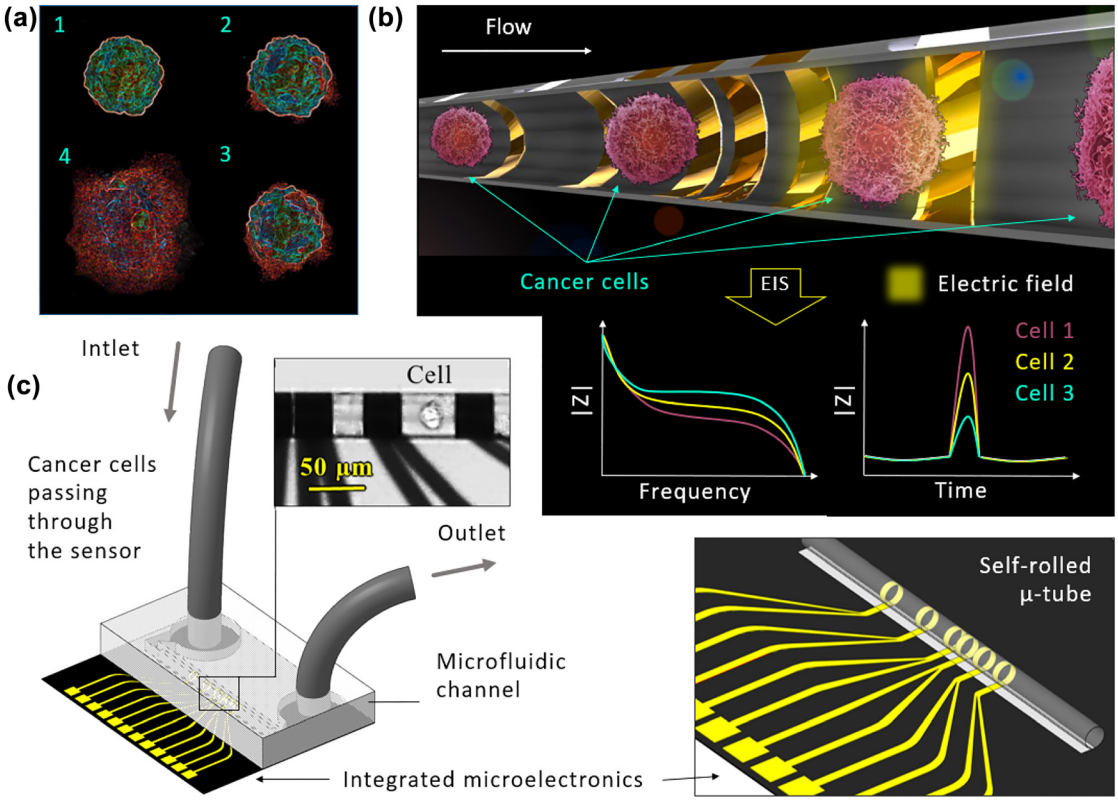

Figure 1: Concept of proposed impedimetric sensor-in-a-tube for single cell analysis: (a) Schematic representation of cancer cell viability changes, (b) single cancer cells passing through the detection electrodes can be analysed in static (impedance spectroscopy) and dynamic modes (single frequency over time), (c) schematic image of proposed sensor-in-a-tube fully integrated into microfluidic channel.

The proposed sensor-in-a-tube is dedicated to single CC cells (HeLa cells) detection and analysis of cell viability upon drug treatment (Camptothecin). During Camptothecin treatment, HeLa cells comes to apoptosis and necrosis through several cell death stages (schematically shown in Figure 1a). Differentiation of initial stages of cell death using conventional µ-TAS and LOC is very challenging because of cells' morphology has very low changes in the beginning of cell death. Deep investigation of cell viability process is a key in development new anti-cancer drugs as well as for the adjustment of conventional medical treatments.

In this work, the detection of HeLa cells and analysis of their viability are processed into self-rolled electrodes in static and dynamic modes by EIS (Figure 1b). Analysis of biological samples in static mode is realized in the frequency range from 10^2 to 5×10^6 Hz. Once, determining the frequency in which the signal-to-noise ratio was the optimal one, single-frequency dynamic mode analysis is then performed, allowing fast flow cytometry. The fabricated sensor-in-a-tube is fully integrated into transparent PDMS microfluidic channel as shown in Figure 1c. Such transparent and oxygen permeable integration helps in stabilizing conditions inside measuring zone, isolate electrodes from analyte and allows optical observation inside the sensing zone.

2 Sensor-in-a-tube fabrication

In the proposed self-rolled approach, we use polymeric materials, which can be photopatterned and whose mechanical and chemical properties can be tuned by modifying them. The full description of polymeric stack fabrication process is described in details elsewhere [29]. In the current paper, we pointed only main steps of sensor fabrication process and the additional optimizations performed for the intended application. Then, three separate layers of polymer were deposited serially one on top of each other to construct the polymer stack. The polymeric stack consists of a sacrificial layer (SL) a pH-sensitive hydrogel (HG) layer (active layer) and a supporting polyimide (PI) layer (passive layer). All polymeric layers were shaped after deposition by photolithography. Detailed information on the employed materials is done in the Experimental section. Once the stack of layer was

prepared, parallel Pt electrodes were patterned onto the PI layer. Finally, the sample was placed into 0.5 M sodium diethylenetriaminepentaacetic acid (DTPA) solution. This solution etches the sacrificial layer and swells the hydrogel simultaneously, resulting in a tube-like structure.

Photolithography of polymeric layers allows fast, precise and cost-effective fabrication process. However, inaccurate tuning of photolithography parameters may lead to formation of links between SL and HG because of incomplete etching of HG form the roughness of SL surface as shown in Figure 2a. Such micro- and nanolinks form small fibers during tube formation and often leads to blocking of tubes' opening and create defects into intertwining space, especially for small inner diameters (below 50 µm). A 10 µm-thick AZ photoresist layer is applied on this step-in order to protect the desired part of polymeric stack from etching (Figure 2a above). All polymeric surfaces outside of the protective layer undergo a complete etching. The total length of the protective layer defines the rolling length of the polymeric stack and, thus, may additionally vary the geometry of the final tube (diameter, number of windings). Therefore, using different layouts of such protective layer allows to change the final geometry of the polymeric stack after preparation. Afterwards, the protective layer is removed by immersing the sample in a Dimethyl sulfoxide bath prior to electrodes sputtering. An example of the produced tubes after oxygen plasma cleaning is shown in Figure 2a, below right. After such optimization and process improvement, a series of parallel tubular electrodes was fabricated with widths of 30 µm, and varying gaps from 5 to 50 µm.

It is also worth noting that DTPA pH and thickness of the polymeric layers have an influence on the final tube diameter and quality, as it was recently reported by our group [29]. Briefly, increase of DTPA pH leads to decrease of final tube diameter because of increased swelling rate. Adversely, increase of PI/HG ratio results in increase of tube diameter. In this paper, polymeric stacks with same thicknesses have been fabricated and rolled in DTPA with pH6, pH8 and pH10 (Figure 2b). Use of pH10 results in the formation of thinner tubes with inner diameters of ca. 30 µm compared to tubes with inner diameter of ca. 100 µm when self-assembling the tubes in DTPA with pH6. In this work, we investigated the influence of different tubes diameters as well as different electrode gap on the sensor-in-a-tube sensitivity.

The resulting sensor-in-a-tube is then integrated within transparent PDMS molded microfluidic chip (Figure 3) by using a conventional mask aligner system and standard oxygen plasma activated bonding. The PDMS mold has a 500 µm-width central channel with two lateral channels from the center to the borders of PDMS mold. Once self-rolled sensor-in-a-tube is aligned inside the central channel and PDMS mold bonded to the glass, the lateral channels are filled with liquid PDMS. Liquid PDMS is then cross-linked by simple heating of whole chip above 100 °C. PDMS filling covers prevent liquid leakages outside the tube. Then, the final chips are connected to a syringe pump via PTFE tubes ($\varnothing_{int.}$ 0.3 mm, $\varnothing_{ext.}$ 0.6 mm) to introduce the analytes for further experiments.

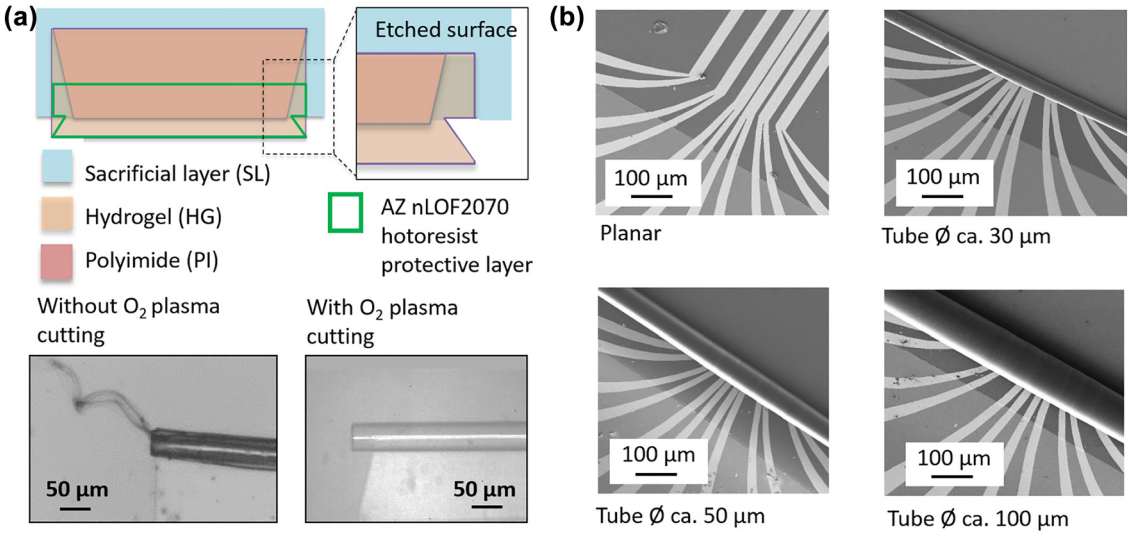

Figure 2: Fabrication of self-rolled tubes: (a) Design of AZ protective layer for polymeric stack cleaning and patterning (above) and examples of self-rolled polymeric tubes without (left) and with (right) plasma cleaning. (b) SEM images of self-rolled tubes with different diameters compared to planar polymeric stack.

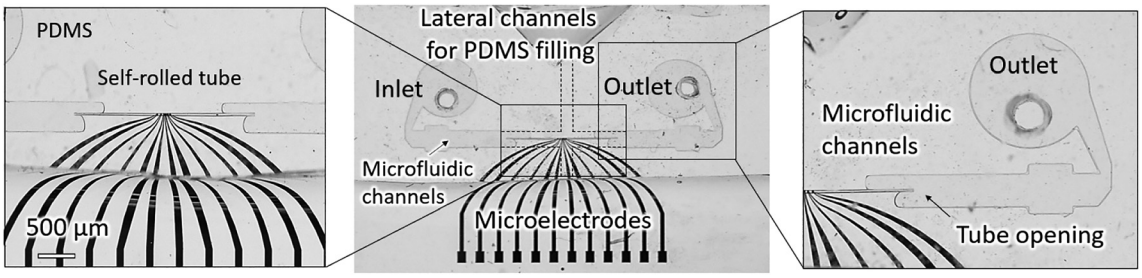

Figure 3: Self-rolled sensor-in-a-tube integrated into PDMS microfluidic channel.

3 Result and discussion

3.1 Sensor calibration

The sensor-in-a-tube is designed for the analysis of cell suspension and single cells. The electrode gap selection is essential to conduct the following investigation of the single cells and extracellular cell medium. Thus, electrode geometry calibration was performed in order to select the appropriate working gap and frequency for higher sensitivity and selectivity. The typical cancer cell size ranges from 20–30 µm, whereas HeLa cervical cancer cells range from 30–40 µm [30]. On another hand, living cells form often cell clusters with different number of cells. Large clusters have negative influence on cell viability because of limiting nutrients in the cluster centre. Such cells cluster or agglomeration is out of scope of present work. Small clusters of 2–3 cells normally forming during cell movement does not affect cell viability and has to be investigated. Based on cancer cell size estimations, the sensor-in-a-tube with working gap between electrodes in ranges 5–50 µm have been fabricated and connected using 4 electrode configuration in order to characterize the influence of the electrode geometry on EIS sensor response (Figure 4a and b). More details are shown in the experimental section.

The impact of the different gaps (from lowest to highest) on the CO_2 independent cell medium's impedance was investigated in static mode in a frequency range from 10^2 to 10^6 Hz (Figure 4c). The impedance signal was more prominent in the higher gaps than the lower ones. For more considerable gap distances, the solution resistance increases proportionally to the distance between the electrodes. Overall, the impedance is then limited by the narrow section's high solution resistance and changes proportionally with the distance between the electrodes. For analysis of single cells, the gap of 50 µm was the most appropriated since it can capture the signal from a single cell and its surrounding medium. Eventual larger gaps require additional flow and cell concentration, precise optimization of analyte since the interelectrode section may often include several cells during the capturing, resulting in the overlapping signal. However, the size of cell clusters is limiting by tube's inner diameter and in present work was set-up at 40–50 µm range corresponding to single cell size.

As the sensor will be used for cell detection purposes, the medium suitable for calibration is the CO_2 independent cell medium. It allows performing the measurements outside the cell incubator, maintaining the cell solution's pH constant. The different cell medium concentrations for

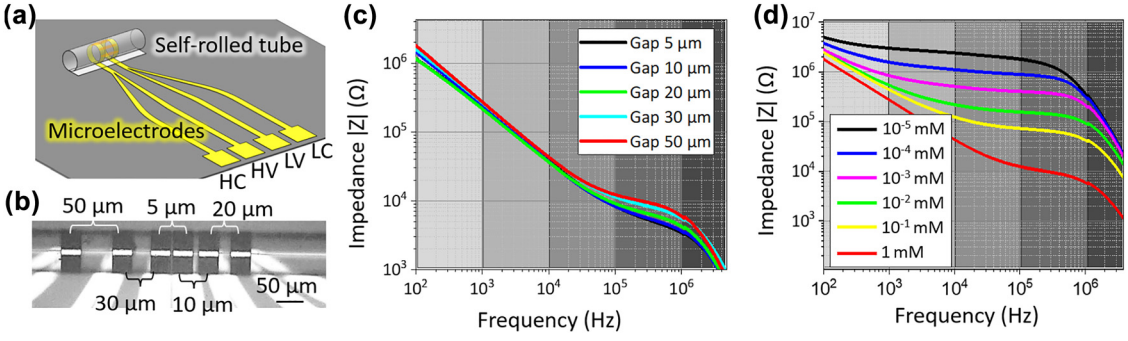

Figure 4: Impedance measurement using microelectrodes with different working distance (gap). (a) Connection scheme. (b) Optical image of the tubular microelectrode shows different electrode gaps. (c) Impedance spectra of CO_2 independent cell medium measured with different gaps. (d) Impedance spectra of CO_2 independent cell medium measured in concentration range from 10^{-5}–1 mM at gap 50 µm.

these measurements were from 10^{-5}–1 mM in the tube of diameter of 40 µm. Impedance spectra of different concentration of CO_2 independent cell medium measured on gap 50 µm showing in Figure 4d indicating increase of the medium conductivity and decrease of impedance during increase of cell medium concentration. This trend is related to the decrease of ionic conductivity due to diluting the initial cell medium in DI water. Thus, the proposed sensor-in-a-tube has the highest impedance amplitude at a frequency of 10^5 Hz which could be used for the subsequent dynamic analysis.

3.2 Flow cytometry

The sensor-in-a-tube has been calibrated in a cell counter dynamic regime for detecting HeLa cells and distinguish different cell types (e.g. single cells, clusters or fragments) presenting in cell suspension (Figure 5a). The external tube attached to the microfluidic channel's inlet is connected to a syringe pump to maintain the constant fluid flow of 0.03 µL/s in sensor-in-a-tube with inner diameter of 40 µm. The concentration of the HeLa cells suspension was 5.7×10^5 cells/mL. According to the above-mentioned static impedance analysis, the excitation frequency of 10^5 Hz is selected for cell detection since the higher impedance response has been recorded at this frequency for single cells. Therefore, keeping the frequency, flow rate, temperature, and electrode gap constant, the cell detection measurements were carried out. As shown in Figure 5b, the peaks are overlapping at higher concentrations, making analysis more difficult compared to the lower concentration of cell suspension. Thus, preliminary dilution of cell suspension could be very easy and effective step towards increasing sensor selectivity and sensitivity.

As mentioned earlier, the EIS analysis can differentiate single cells, clusters, and cellular debris or fragments. Figure 5b indicates the signal of clusters, single cells and debris with respect to the baseline and can be represented in a form of cloud graph (Figure 5c). Approximately, 55 single cells and 5 clusters have been selected and plotted in this graph. Correspondence of peaks with different cell types was done by optical visual control through transparent PDMS encapsulation in real time (Figure 5d).

3.3 Cell viability analysis

Cell viability is defined as the number of healthy cells present in the cell suspension/culture with respect to the

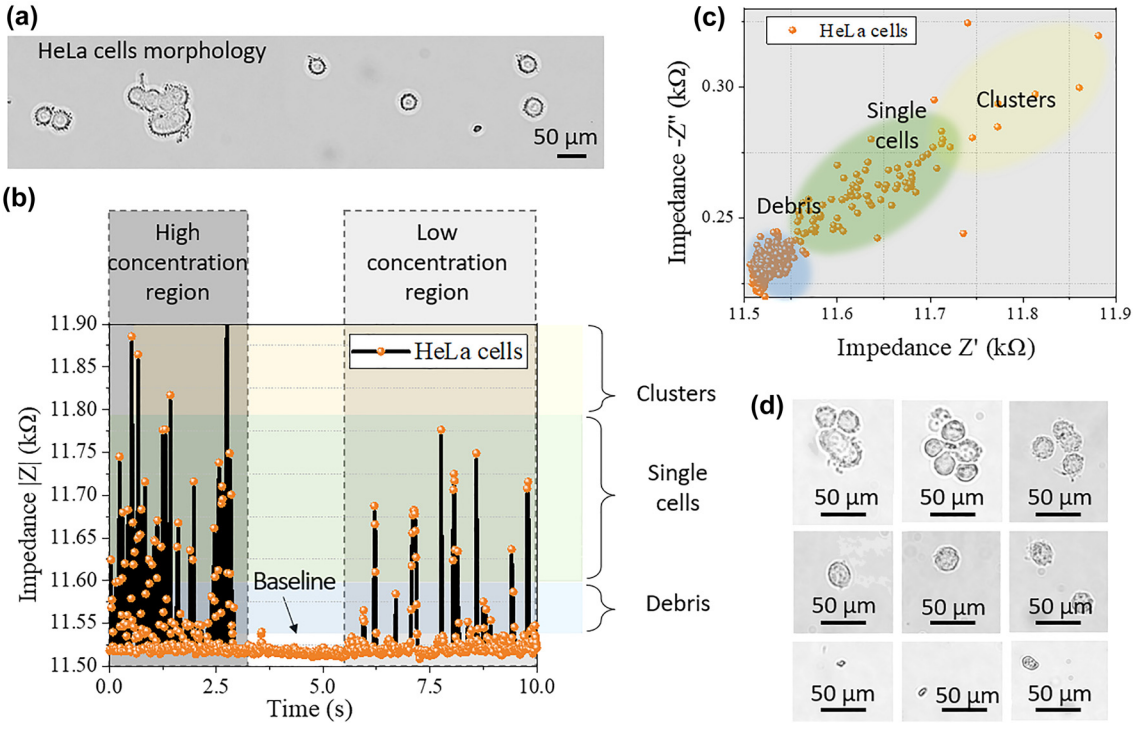

Figure 5: HeLa cells flow cytometry measured at 10^5 Hz with an electrode gap of 50 µm and a tube diameter of 40 µm. (a) Optical microscopy image of typical morphologies of HeLa cells in cell suspensions. (b) Chronoimpedance of HeLa cells suspensions at to different concentration regions, respectively: High and low concentration. (c) The analytical cloud graph of single cells, cluster and debris, showing both the imaginary and real part of the impedance of ca. 200 samples, in which three different regions can be easily distinguished, namely: Single cells, cell clusters and cellular debris. (d) Optical microscopy of different cell types: Clusters, single cells, cell debris or fragments.

whole cell population. Cell viability is an essential factor to evaluate the effectiveness of the applied drugs. Cancer cells' death is a complex process related to the release of ions and proteins from the cytoplasm, changing the extracellular medium's electrical properties. Likewise, cells experience changes in the membrane surface such as charge or polarization, both being detectable by EIS analysis [31]. Cell death can occur by apoptosis, which is generally triggered by normal, healthy processes, and by necrosis which is triggered by external factors or diseases [5]. Therefore we carried out experiments with HeLa cells treated by two means: one incubating the cells in DI water for 6 and 24 h, and by incubating them with different concentrations of Camptothecin, the chosen anticancer drug.

First, we evaluated the cell viability when treating the cell samples with DI water during different periods of time, achieving survival rates of 20, 60 and 100%, estimated by a cell viability assay (details in the Experimental section). Optical fluorescent imaging of the treated cells is shown in Figure 6. As observed in the same picture, in the brightfield images it was not possible to distinguish evident changes in cell morphology. Thus, by applying the same treatment, we measurde the three different cell populations using EIS to correlate the data (Figure 7a).

As expected, there is a decrease in the amplitude of the impedance as the number of dead cells increases. The difference between the control sample (living cells) and the treated cells (dead cells) is visible in the whole frequency range. Treated cell suspension has higher impedance compared to control samples which may be related to release of specific proteins from cells to surrounding medium. According to preliminary measurements, release of cell proteins often leads to an increase of solution impedance [29]. These cell proteins are released by the total cell membrane fragmentation, increasing solution resistance. Treated cells suspensions with ca. 60% and ca. 20% of live cells have a slight decrease in impedance for ca. 20% live cells compared to ca. 60%, which may correspond to the expression of intracellular ions in the cell surrounding medium as well as presents of small amount of water residuals. Cytoplasmic ions presenting in cell suspensions increases medium conductivity especially in case of maximum dead cells. However, static investigation of cell viability by analysis of EIS spectra does not provide sufficient information for precise differentiation of cell viability stages. Alternatively, dynamic peak analysis can provide additional information for cell differentiation.

Dynamic analysis of treated HeLa cells was also performed according to the conditions mentioned above (Figure 7b). The EIS peak amplitudes of cells correspond to the cell membrane polarization or charge. When the cells start to die, the membrane disrupts, causing a rapid depolarization. Thus, the ratio between peak amplitude of cell and solution impedance (SNR) corresponds to cell viability properties. Chronoimpedance investigation of

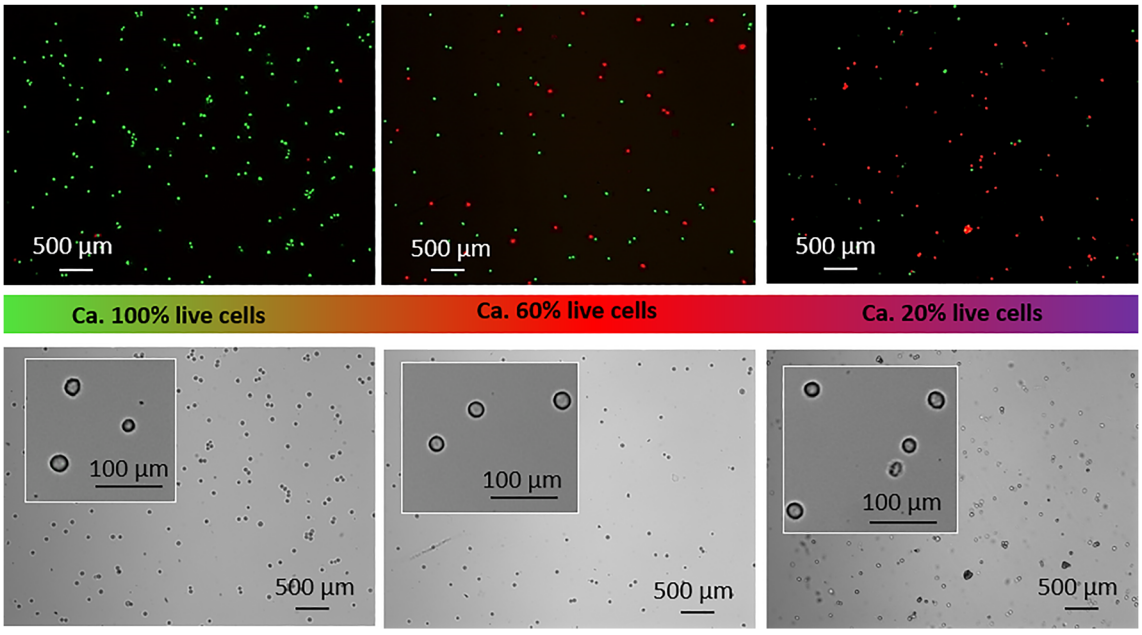

Figure 6: Brightfield and fluorescent visualization of ca. 100, 60 and 20% living HeLa cells after different incubation times in DI water. Live cells display green and dead cells red fluorescence.

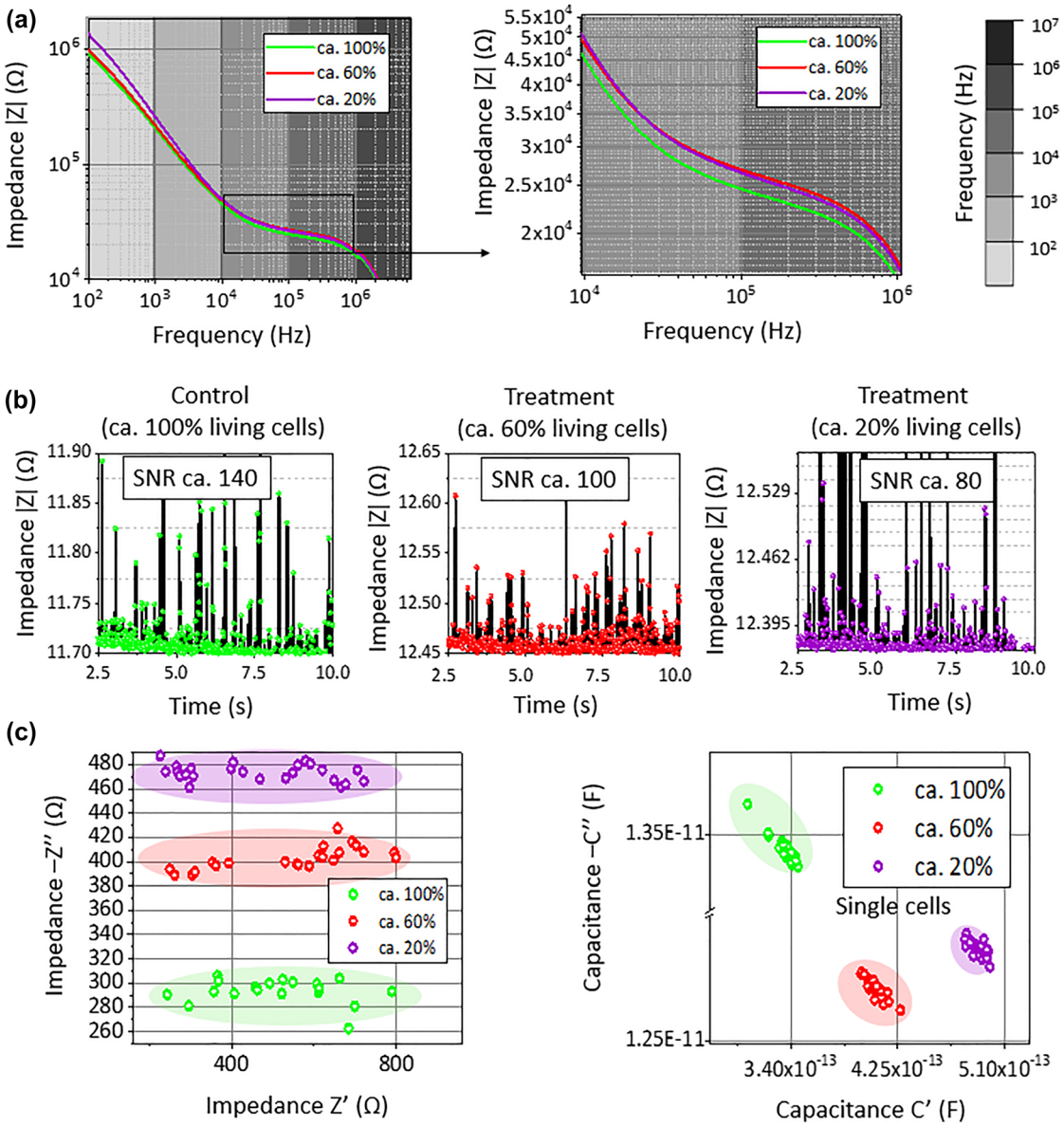

Figure 7: EIS measurements of HeLa cells viability in static and dynamic mode when treated with DI water. (a) Impedance spectra of cell suspension with different number of living cells. (b) Chronoimpedance of HeLa cell suspension with different number of living cells. Only peaks corresponding to single cells are selected and counted to determine SNR. (c) Cloud graphs representing different viability stages.

treated HeLa cells shows clear tendency of decreasing SNR from ca. 100 for ca. 60% living cells to ca. 80 for ca. 20% living cells. This depolarization trend of the single cell's membrane is also observed in cloud graphs of complex values of impedance capacitance (Figure 7c). Combination of static and dynamic analyses permits to gather data from the cell surrounding medium and single cells which can be crucial for complex cell differentiations e.g. treatment of cancer cells with different concentrations of anti-cancer drugs.

3.4 Anti-cancer drug treatment investigation

The sensor-in-a-tube is now used to distinguish between the different stages of the cancer cells death i.e. apoptosis and necrosis, at a single cell level with high throughput. This differentiation could provide additional information on high toxicity of drug agents in cancer patients. The Camptothecin has been used as a model drug in the present work. Camptothecin is a well-known anti-cancer drug with proven

effectiveness [5]. In this work, it has been used to detect the cell death mechanisms at a single cell level, which helps improve drug therapies and develop new drugs.

HeLa cells have been exposed to different concentrations of Camptothecin solution (from 0 to 100 mg/mL), and then washed in CO_2 independent cell medium to remove the residual drug and resuspended in a new cell medium. Fluorescence microscopy images showing the cell viability upon treatment with different drug concentrations are shown in Figure 8a. In the reference sample (without drug treatment), almost all cells are alive during measurements. Then, with the increase in drug concentration, more cells start to die by apoptosis. From the concentration of 0.5 mg/mL, more cells are utterly dead by apoptosis and necrosis. The treated cells were also measured using EIS. The resulting bode impedance plot (Figure 8b) reveals no significant difference among the cell suspension when using different drug concentrations. However, when using the complex impedance and complex capacitance cloud graphs (Figure 8c), it is clearly observed that there is a significant increase in signal for the highest drug concentrations (10 and 100 mg/mL) and small differences in the signal for the concentration range of 0.5–0.1 mg/mL. Based on this response over the whole frequency range, we performed single cell in-flow analysis which allowed to perform more in-depth investigation on the cell-dead over time, based on the analysis of cell membrane polarization. The SNR diagram for different Camptothecin concentrations is shown in Figure 8c right. The SNR decrease correlated with the cell death is shown according to previous results. However, there are two regimes which can be noticed: decreased SNR for the concentration range of 0.05–0.1 mg/mL and 0.5–100 mg/mL. Between these two concentration ranges, the SNR increases from ca. 40 to ca. 60. It is assumed that this transition can be associated with the changes in the cell death mechanism from apoptosis to necrosis. However, at the current stage it is difficult to confirm this claim. Further studies and additional measurements need to be pursued in order to confirm these results.

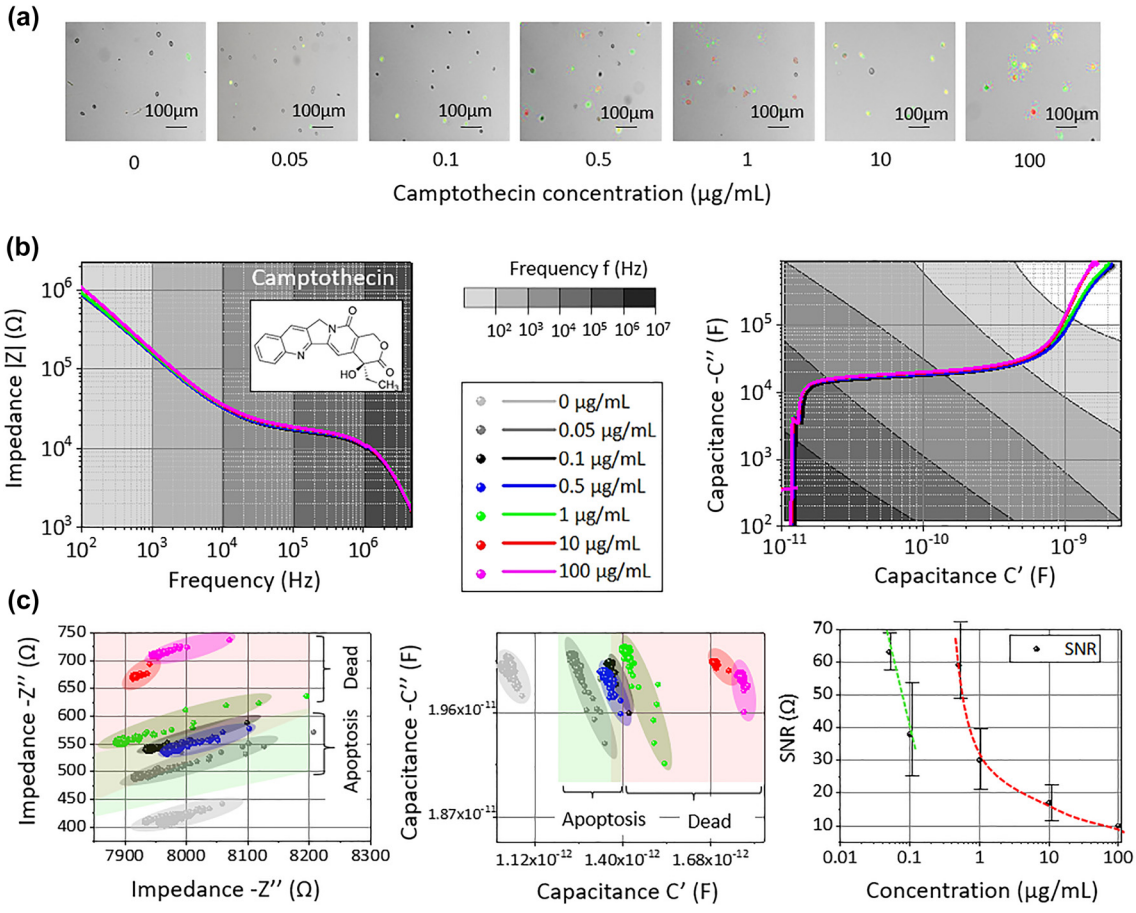

Figure 8: EIS measurements of anti-cancer drug treated HeLa cells. (a) Optical fluorescent image of the cells after treating with the camptothecin of concentration ranging from 0 to 100 mg/mL. (b) Impedance spectra and complex capacitance plot of HeLa cells suspension treated with camptothecin in a concentration range from 0 to 100 mg/mL. (c) Complex impedance and complex capacitance cloud plots of signals detected from single HeLa cells and graphical representation of SNR measured on single HeLa cells treated with camptothecin.

4 Experimental section

4.1 Fabrication details

A $100 \times 100 \times 1\,mm^3$ glass slide is used for the substrate. It is evident to choose glass as a substrate candidate because it is inexpensive and compatible with the micrometer sculpturing. The static chemical nature of the material makes it suitable for the massive production of devices. Glass substrates were first silanized using organofunctional alkoxysilane molecules to produce a strong chemical bonding between the mineral substrate and the adhesives' organic components. The polymeric stack consist of a sacrificial layer (SL) was spin-coated to produce a 500 nm thick layer. Then, the photosensitive hydrogel (HG) is deposed by spin-coating as a second layer, which acts as an active layer because of its unique swelling characteristics. Finally, the supporting polyimide (PI) layer was deposed on top of previous layer. All polymeric layers were shaped after deposition by photolithography. Once the stack of layer was prepared, parallel Pt electrodes were patterned onto the PI layer Prepared polymeric stack was finalized by sputtering of Pt microelectrodes onto PI layer.

After completing the tubular device's encapsulation, the devices are ready for the subsequent impedance measurements. The impedance measurement is done using Agilent 4294A precision impedance analyzer. The electrodes of the sample are connected in four-probe configuration with Cascaded Microtech DCP 100 probes (FormFactor) on the PSM 6 wafer probe station (Karl Suss). The constant temperature of 37 °C was maintained with the help of a Peltier element. As per the 4-probe configuration, 3D tubular microelectrodes' contact pads are connected to high voltage (HV), high current (HC), low voltage (LV), and low current (LC), as shown in Figure 4a.

4.2 Cell culturing and staining process

The medium used for the cells consists of the composition of DMEM (D5671 from Sigma), 10% FCS, 1% Penicillin/Streptomycin, and 1% L-Glutamine. The cells are split every 3–4 days. For splitting, the cells are washed with PBS for removing the medium. Then Trypsin is added, which is the enzyme used to break the extracellular proteins. It is mainly used to detach adherent cells from the bottom of the culture dishes. To inactive this enzyme, the medium is added. The cells are then transferred into a 1.5 mL falcon tube. Before removing the medium again, the cells are centrifuged for 5 min. The cells are resuspended in 1 mL medium. The cells are seeded in 150 µL (1:7) into a new culture flask. Finally, the cells are cultured at 5% CO_2 and 37 °C. For the measurement, the cells are counted with a Neubauer Haemocytometer.

The 500 µL of living cells are diluted with 500 µL of CO_2 independent medium in a 2 mL falcon tube. Then, kept in the incubator at 37 °C. In another two 2 mL falcon tube, 500 µL of living cells added with 500 µL of water is kept at 50 °C in each tube. One tube was kept for 6 h and the other one for 24 h to kill the cells. After 6 h, both the living and the supposed dead cells are centrifuged for 3 min, and then the medium was removed. After the centrifuge, it has been observed that cells are at the bottom of the falcon tube, forming a white pellet-like structure. The medium is carefully removed without harming the cells which are at the bottom of the tube. Now the medium is changed with the cell medium and is ready for measurement. The same procedure is followed for the dead cells, which are kept for 24 h. For staining, 200 µL is taken from each of the two bottles of living and dead cells, and 2 µL of SYBER 14 dye from the LIVE/DEAD Sperm Viability kit is added to them. Both the living and dead cells are incubated for 5 min at 37 °C. After 5 min s, 2 µL of Propidium iodide is added to the same cells and again incubated for 5 min at 37 °C. The cells are finally ready for imaging in the cell observer. The imaging and measurements were carried out simultaneously with a AxioTech Vario, Carl Zeiss Microscopy GmbH microscope to acquire the accurate measurement results of the cell viability.

5 Conclusions

A novel impedimetric microfluidic sensor-in-a-tube for label-free single tumor cells analysis is introduced. The sensor is fabricated for the simultaneous detection of single cells and extracellular cell medium, in static and dynamic modes, over an excitation frequency range from 10^2 to 5×10^6 Hz, without employing functionalization and labelling strategies. The analysis platform is based on a self-assembled strained polymeric layer stack containing Pt electrodes, forming a rolled-up microelectrode with a diameter close to the cancer cell size. These rolled-up platinum microelectrodes are integrated into a microfluidic channel which also improve the SNR and reduce significantly the volume of sample and reagents required. In order to identify the sensitivity, the sensor has been calibrated with different concentrations of cell medium. Additionally, the EIS response has been investigated on electrode configuration with multiple gaps (5 to 50 µm). Among these gaps, the gap of 50 µm was selected due to the size corresponding single cell and surrounding medium to be analysed. Model cancer cells (HeLa cells) with concentration of 5.7×10^5 cells/mL have been successively detected in dynamic mode. Optical microscopy imaging was used to calibrate the developed sensor-in-a-tube, allowing to distinguish among single cells, cell clusters, and cellular debri, by EIS. The impedimetric signal of treated and untreated cancer cells were in good agreement with the fluorescence microscopy images, showing similar rates of cell survival according to the applied treatment. Static analysis when treated the cancer cells with DI water, revealed an increase of impedance for both ca. 20% and ca. 60% of living cells compared to ca. 100% associated more likely with cell medium's cellular proteins and metabolism products. Ca. 20% of living cells sample has decreased impedance than ca. 60% of living cells, probably due to cytoplasm release into the extracellular medium during cell death. Along with the cell viability monitoring, we aimed to distinguish between the apoptosis and necrosis phenomena of the dead cells upon Camptothecin (anti-cancer drug) treatment at concentrations of

0.05 mg/mL, 0.1 mg/mL, 0.5 mg/mL, 1 mg/mL, 10 mg/mL, 100 mg/mL. The sensor-in-a-tube was able to identify cell death (mainly by apoptosis) in a low concentration range (0.05 to 0.1 mg/mL). Nevertheless, starting from 0.5 mg/mL, cell death seems to result in a different impedance response, which we assume is due to a different cell dead mechanism: necrosis, as in previous studies, reports on cell necrosis when employing higher doses of Camptothecin has been demonstrated [5]. Here, we suggest a single cell in-flow analysis as a tool for investigation and distinguishing dead cell behavior. We believe that this 3D impedimetric microfluidic rolled-up sensor could potentially be the next generation analytical system and can be used for the rapid point-of-care diagnosis for cancer cells and for personalized drug screening.

Acknowledgements: O.G.S. acknowledges financial support by the Leibniz Program of the German Research Foundation (SCHM 1298/26-1). M. Medina-Sánchez acknowledges financial support by the European Union's Horizon 2020 research and innovation program (Grant agreement No. 853609). The authors warmly thank F. Hebenstreit for the biological experiment's assistance. The support of the clean room team headed by R. Engelhard and the assistance in development of the experimental setups by the research technology department of IFW Dresden is greatly appreciated. We further thank C. Krien and I. Fiering for the deposition of metallic thin films, F. Striggow for SEM analysis.

Author contributions: All the authors have accepted responsibility for the entire content of this submitted manuscript and approved submission.

Research funding: The work was financially supported by the German Research Foundation DFG SPP 1857 ESSENCE grant (KA5051/1-1 and ME4868/2-1).

Conflict of interest statement: The authors declare no conflict of interest.

References

[1] M. Vu, J. Yu, O. A. Awolude, and L. Chuang, "Cervical cancer worldwide," *Curr. Probl. Cancer*, vol. 42, no. 5, pp. 457–465, 2018.

[2] World Health Organization, *WHO Guideline for Screening and Treatment of Cervical Pre-cancer Lesions for Cervical Cancer Prevention: Use of mRNA Tests for Human Papillomavirus (HPV)*. 2nd ed., 2021, [Online]. Available at: https://www.who.int/publications/i/item/9789240030824.

[3] N. Wentzensen, M. Schiffman, T. Palmer, and M. Arbyn, "Triage of HPV positive women in cervical cancer screening," *J. Clin. Virol.*, vol. 76, pp. S49–S55, 2016.

[4] A. Saadatpour, S. Lai, G. Guo, and G. C. Yuan, "Single-cell analysis in cancer genomics," *Trends Genet.*, vol. 31, no. 10, pp. 576–586, 2015.

[5] A. Z. Mirakabadi, A. Sarzaeem, S. Moradhaseli, A. Sayad, and M. Negahdary, "Necrotic effect versus apoptotic nature of Camptothecin in human cervical cancer cells," *Iran. J. Cancer Prev.*, vol. 5, no. 3, pp. 109–116, 2012.

[6] J. Wu, M. Dong, C. Rigatto, Y. Liu, and F. Lin, "Lab-on-chip technology for chronic disease diagnosis," *npj Digit. Med.*, vol. 1, no. 1, pp. 1–11, 2018.

[7] B. Sharma and A. Sharma, "Microfluidics: recent advances toward lab-on-chip applications in bioanalysis," *Adv. Eng. Mater.*, vol. 24, no. 2100738, 2022.

[8] C. D. Ahrberg, A. Manz, and B. G. Chung, "Polymerase chain reaction in microfluidic devices," *Lab Chip*, vol. 16, no. 20, pp. 3866–3884, 2016.

[9] A. Joshi, A. Vishnu, T. Sakorikar, A. M. Kamal, J. S. Vaidya, and H. J. Pandya, "Recent advances in biosensing approaches for point-of-care breast cancer diagnostics: challenges and future prospects," *Nanoscale Adv.*, vol. 3, no. 19, pp. 5542–5564, 2021.

[10] J. Suikkola, T. Björninen, M. Mosallaei, et al., "Screen-printing fabrication and characterization of stretchable electronics," *Sci. Rep.*, vol. 6, no. May, pp. 1–8, 2016.

[11] J. Izdebska, "Printing on polymers: fundamentals and applications print." *Polym. Fundam. Appl.*, no. July, 2015, pp. 1–424.

[12] V. Narayanamurthy, Z. E. Jeroish, K. S. Bhuvaneshwari, et al., "Advances in passively driven microfluidics and lab-on-chip devices: a comprehensive literature review and patent analysis," *RSC Adv.*, vol. 10, no. 20, pp. 11652–11680, 2020.

[13] G. Dutta, J. Rainbow, U. Zupancic, S. Papamatthaiou, P. Estrela, and D. Moschou, "Microfluidic devices for label-free DNA detection," *Chemosensors*, vol. 6, no. 4, 2018, https://doi.org/10.3390/chemosensors6040043.

[14] Q. Hassan, S. Ahmadi, and K. Kerman, "Recent advances in monitoring cell behavior using cell-based impedance spectroscopy," *Micromachines*, vol. 11, no. 6, 2020, https://doi.org/10.3390/MI11060590.

[15] L. L. Crowell, J. S. Yakisich, B. Aufderheide, and T. N. G. Adams, "Electrical impedance spectroscopy for monitoring chemoresistance of cancer cells," *Micromachines*, vol. 11, no. 9, 2020, https://doi.org/10.3390/mi11090832.

[16] Y. Feng, L. Huang, P. Zhao, F. Liang, and W. Wang, "A microfluidic device integrating impedance flow cytometry and electric impedance spectroscopy for high-efficiency single-cell electrical property measurement," *Anal. Chem.*, vol. 91, no. 23, pp. 15204–15212, 2019.

[17] A. Sun, A. G. Venkatesh, and D. A. Hall, "A multi-technique reconfigurable electrochemical biosensor: enabling personal health monitoring in mobile devices," *IEEE Trans. Biomed. Circuits Syst.*, vol. 10, no. 5, pp. 945–954, 2016.

[18] J. Cottet, A. Kehren, H. van Lintel, F. Buret, M. Frénéa-Robin, and P. Renaud, "How to improve the sensitivity of coplanar electrodes and micro channel design in electrical impedance flow cytometry: a study," *Microfluid. Nanofluidics*, vol. 23, no. 1, 2019, https://doi.org/10.1007/s10404-018-2178-6.

[19] L. Wang, L. A. Flanagan, N. L. Jeon, E. Monuki, and A. P. Lee, "Dielectrophoresis switching with vertical sidewall electrodes for microfluidic flow cytometry," *Lab Chip*, vol. 7, no. 9, pp. 1114–1120, 2007.

[20] S. Choi and J. K. Park, "Microfluidic system for dielectrophoretic separation based on a trapezoidal electrode array," *Lab Chip*, vol. 5, no. 10, pp. 1161–1167, 2005.
[21] Y. Yu, J. Chen, and J. Zhou, "Parallel plate lab on a chip based on digital microuidics for on-chip electrochemical analysis," *J. Micromech. Microeng.*, vol. 24, no. 1, 2014, https://doi.org/10.1088/0960-1317/24/1/015020.
[22] G. Kang, S. K. Yoo, H. I. Kim, and J. H. Lee, "Differentiation between normal and cancerous cells at the single cell level using 3-D electrode electrical impedance spectroscopy," *IEEE Sensor. J.*, vol. 12, no. 5, pp. 1084–1089, 2012.
[23] M. Ibrahim, J. Claudel, D. Kourtiche, and M. Nadi, "Geometric parameters optimization of planar interdigitated electrodes for bioimpedance spectroscopy," *J. Electr. Bioimpedance*, vol. 4, no. 1, pp. 13–22, 2013.
[24] S. M. Weiz, M. Medina-Sánchez, and O. G. Schmidt, "Advanced biosystems – microsystems for single-cell analysis.pdf," *Adv. Biosys.*,vol. 2, no. 1700193, 2018.
[25] E. J. Smith, W. Xi, D. Makarov, et al., "Lab-in-a-tube: ultracompact components for on-chip capture and detection of individual micro-/nanoorganisms," *Lab Chip*, vol. 12, no. 11, pp. 1917–1931, 2012.
[26] C. S. Martinez-Cisneros, S. Sanchez, W. Xi, and O. G. Schmidt, "Ultracompact three-dimensional tubular conductivity microsensors for ionic and biosensing applications," *Nano Lett.*, vol. 14, no. 4, pp. 2219–2224, 2014.
[27] M. Medina-Sánchez, B. Ibarlucea, N. Pérez, et al., "High-performance three-dimensional tubular nanomembrane sensor for DNA detection," *Nano Lett.*, vol. 16, no. 7, pp. 4288–4296, 2016.
[28] C. S. Bausch, C. Heyn, W. Hansen, et al., "Ultra-fast cell counters based on microtubular waveguides," *Sci. Rep.*, vol. 7, pp. 1–11, 2017.
[29] A. I. Egunov, Z. Dou, D. D. Karnaushenko, et al., "Impedimetric microfluidic sensor-in-a-tube for label-free immune cell Analysis," *Small*, vol. 17, no. 2002549, 2021.
[30] J. C. Mijn, K. W. Eng, P. Chandra, et al., "The genomic landscape of metastatic clear cell renal cell carcinoma after systemic therapy," *Mol. Oncol.*, vol. 16, pp. 2348–2395, 2022.
[31] A. Susloparova, D. Koppenhöfer, X. T. Vu, M. Weil, and S. Ingebrandt, "Impedance spectroscopy with field-effect transistor arrays for the analysis of anti-cancer drug action on individual cells," *Biosens. Bioelectron.*, vol. 40, no. 1, pp. 50–56, 2013.